Hole mobilities in films of a pyrazoline:polycarbonate molecularly doped polymer

A. Peled,* L. B. Schein, and D. Glatz
IBM Research Division, Almaden Research Center, 650 Harry Road, San Jose, California 95120-6099
(Received 30 October 1989)

The hole mobilities μ of solution cast 1-phenyl-3-*p*-diethylaminostyryl-5-*p*-diethylphenyl-pyrazoline:polycarbonate (DEASP:PC) thin films have been characterized by the time-of-flight technique. The mobilities were measured for DEASP doping concentrations in the range 10–90 % over a wide range of temperatures and electric fields, including measurements above the glass transition temperature T_g, and analyzed with use of recently suggested deconvolution procedures. The independence of the activation energy on the calculated distance between DEASP molecules ρ and the exponential dependence of μ on ρ suggest nonadiabatic small-polaron hopping is occurring, as was concluded for the molecularly doped polymer hydrazone:PC. The decrease in activation energy above the glass transition temperature is clear evidence of the role of the polymer matrix in determining the activation energy. The electric-field dependence of μ, while similar to previous measurements, i.e., $\ln\mu \propto \sqrt{E}$, provides significant new information. We report the first characterization of the field dependence of μ above the glass transition temperature: It appears to be unaffected by T_g, in contrast to the behavior of the activation energy. We also report the first observation of a mobility that decreases as the electric field increases at 10% DEASP concentration above 370 K. This result is contrary to the predictions of several investigators, but consistent with empirical equations suggested earlier.

I. INTRODUCTION

Charge transport in molecularly doped polymers (MDP) has been a subject of continuous investigation over the past 20 years because of its importance to fundamental charge-transport studies in amorphous materials and its applications in electrophotography.[1] While several amorphous organic MDP films have been thoroughly investigated,[2–9] the experimental characterization of the charge mobility has not resulted yet in an acceptable comprehensive physical model of the processes involved in charge transport.

Common features are observed in these systems. For example, all charge-carrier-mobility data obtained to date can be fit with the empirical equation

$$\mu(T,E,\rho)=\mu_0\exp(-\Delta_0/kT) \times\exp\left[\beta E^{1/2}\left[\frac{1}{kT}-\frac{1}{kT_0}\right]\right], \quad (1)$$

where $\mu(T,E,\rho,)$ is the drift mobility as a function of temperature T, electric field E, and intramolecular distance ρ, and k is Boltzmann's constant. μ_0 is the mobility value at $E=0$ and $T\rightarrow\infty$, and usually depends exponentially on ρ:

$$\mu_0=a_0\rho^2\exp(-2\rho/\rho_0), \quad (2)$$

where a_0 is a constant and ρ_0 describes the decay of the electron wave function. β and T_0 are parameters that characterize the electric field dependence of μ. Note that the electric field is raised to the $\frac{1}{2}$ power. While workers have reported this exponent to vary from $\frac{1}{2}$ to 1, a recent thorough mathematical analysis[10] has confirmed $\frac{1}{2}$ to be the best fit. Δ_0 is the zero electric field activation energy; presumably it represents the activation energy required for hopping. Recent work suggests that this is half the polaron binding energy.[5] ρ is the calculated average isotropic distance between the dopant molecules. This isotropic assumption, however, is not strictly justified from a microscopic point of view since the calculated values of ρ are on the order of the size of the highly asymmetric molecules. However, one may regard the calculated value of ρ simply as an alternative, equivalent specification of the dopant molecular concentration.

It is the purpose of this work to investigate thoroughly another MDP, DEASP:PC (1-phenyl-3-*p*-diethylaminostyryl-5-*p*-diethylphenyl pyrazoline in polycarbonate) whose chemical structure is given in Fig. 1, in an

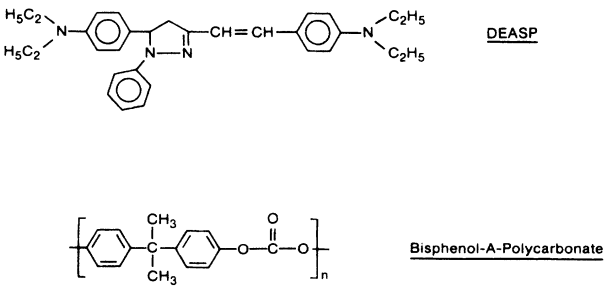

FIG. 1. Structures of DEASP and bisphenol-*A*-polycarbonate (M60, Mobay Chemical Corporation).

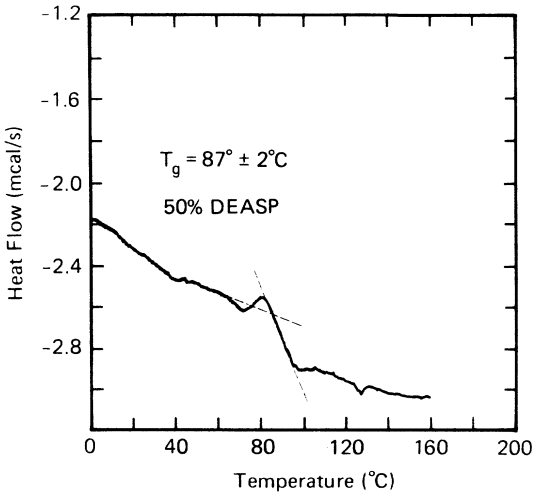

FIG. 2. A typical differential scanning calorimetry (DSC) curve for a 50% DEASP:PC sample; $T_g = 360$ $T_g = 360$ K.

attempt to obtain experimental data over wide E, T, and ρ ranges to be correlated with available electrical hopping theores in amorphous photoconductors. In particular, data above as well as below the glass transition temperature T_g are presented. Initial measurements[11] showed an interesting phenomenonon for the low 10% DEASP concentration: the drift mobility decreased as the electrical field increased above 370 K. In this paper we present a more comprehensive characterization of the DEASP:PC system and compare it to previously investigated MDP systems. The data, after deconvolution, suggest that DEASP:polycarbonate is an example of nonadiabatic small polaron hopping. However, the electric field dependence of the mobility, while consistent with prior measurements in MDP's, is inconsistent with the predictions of all hopping theories.

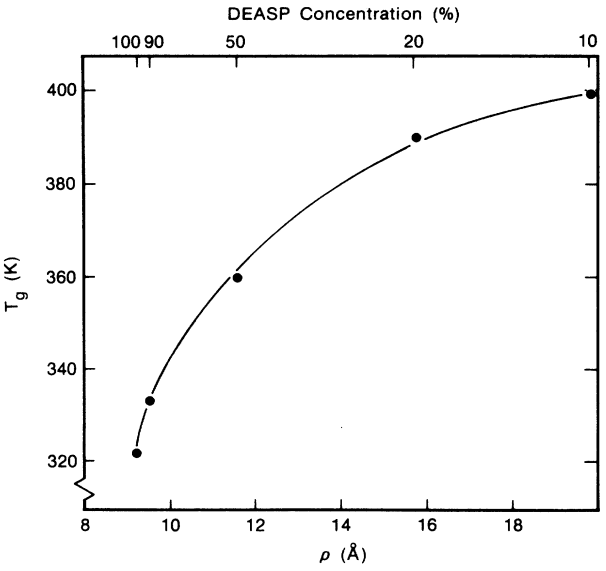

FIG. 3. Glass transition temperature T_g vs intramolecular spacing in DEASP:PC for the range 10–100 % obtained from DSC scans.

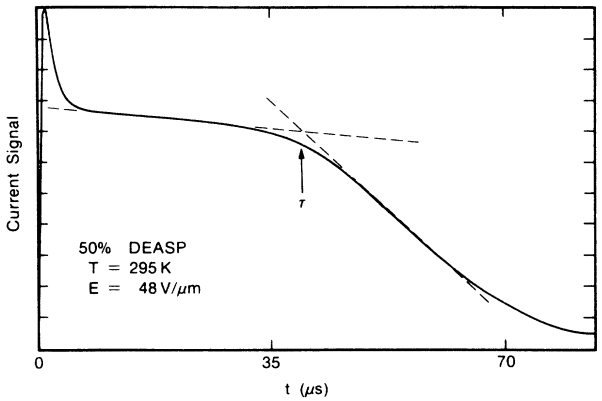

FIG. 4. Typical current transient wave form in TOF experiments.

II. EXPERIMENT

DEASP [a pyrazoline derivative,[12] (see Fig. 1)] and PC (M60, a polycarbonate obtained from Mobay Chemical Corporation) were dissolved in tetrahydrofuran (THF). The solution was cast onto aluminized poly(ethyleneterephtalate) (Mylar) substrates using the doctor-blade technique to obtain thin films in the 5–15-μm thickness range. The resulting wet films were dried and thermally aged in a vacuum oven for 48 h at 40 °C. The doping concentration of the samples was varied in the range of 10–90% by weight DEASP in PC. A thin blocking layer of (500 Å) of SiO was vacuum deposited directly onto the MDP films. A top conductive electrode of Au was deposited on the blocking layer with a nominal area of 1 cm^2. The sample thickness was determined by capacitance measurements, calibrated by physical thickness measurements using thick samples (≈ 30 μm) and a Fowler Digitrix II micrometer. No crystallization could be observed

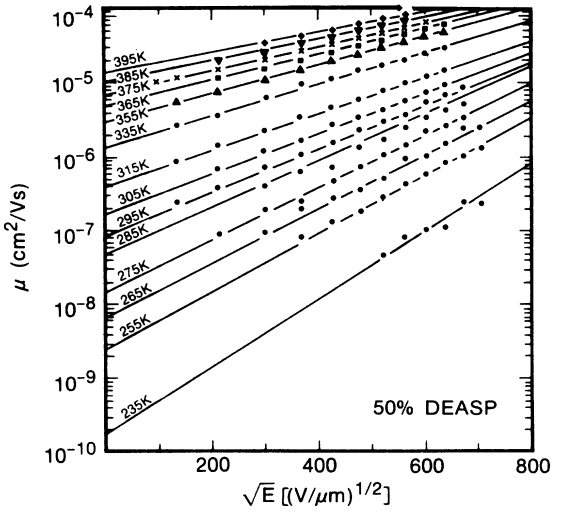

FIG. 5. Logarithm mobility vs square root of the electric field for 50% DEASP:PC. The family of curves is for various temperatures in the range 235–395 K; T_g is 360 K for this sample.

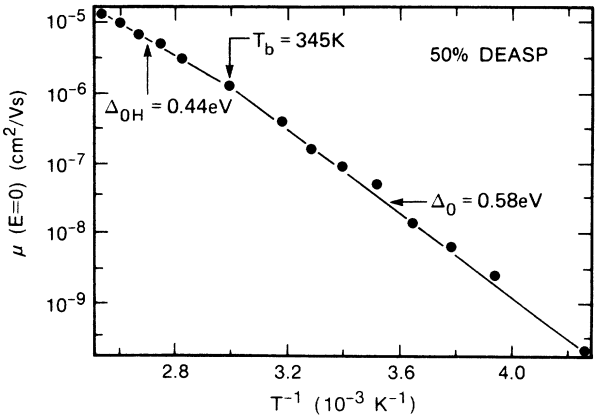

FIG. 6. Logarithm plot of zero field mobility taken from Fig. 5 vs temperature for 50% DEASP:PC.

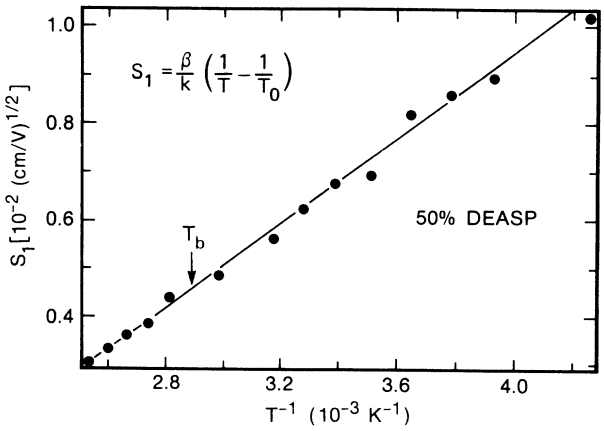

FIG. 8. Plot of the slope of the curves given in Figs. 5, $S_1(T)$, vs inverse of temperature for 50% DEASP:PC.

in any of the samples prepared by visual inspection or (DSC) analysis for the whole 10–90 % DEASP concentration range. Spectrometric analyses were employed to confirm that the weighted concentrations of DEASP:PC was within a ±1% accuracy. The glass transition temperature T_g was determined from DSC experiments for which a typical curve is shown in Fig. 2 (for 50% DEASP:PC). The solid T_g curve versus concentration of DEASP in PC was obtained for the range of 10–100 % and is displayed in Fig. 3.

The mobility measurements were performed by the time-of-flight (TOF) technique described earlier.[5] The electrical drift mobility was calculated from the transit times computed from digitized current wave forms (see details in Ref. 5). The current pulses were recorded for the widest temperature and electric field ranges possible, requiring that the traces showed clear evidence of a transit time on linear current-time axes. During the measurements care was exerted to avoid space-charge effects and to optimize the amount of charge carriers generated by the laser flash with respect to the signal-to-noise ratio.

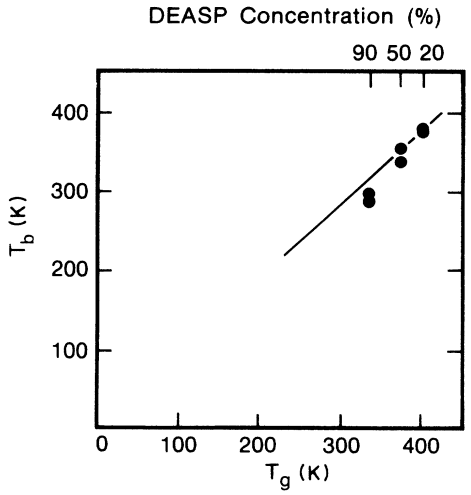

FIG. 7. Plot of the electrically obtained temperature parameter T_b against the glass transition temperature T_g.

Figure 4 shows a typical transient current trace for a 90% DEASP:PC sample at $T=295$ K and $E=48$ V/μm. The highest fields used were determined by the sample's breakdown voltage at high temperature. The breakdown voltage itself was found to be dependent on temperature and only slightly upon the dopant concentration. The mobility measurements were performed for 10, 20, 50, and 90 % concentrations of DEASP:PC. For each concentration typically 2–3 samples taken from different sheets were measured throughout similar ranges of voltage and temperature. The results were reproducible to a degree which will appear clearly in the experimental plots. No hysteresis of the mobility values was observed when the temperature was raised to the highest temperature and lowered back to room temperature. The calculated parameters are shown in most graphs as 2 points representing measurements taken from two different sam-

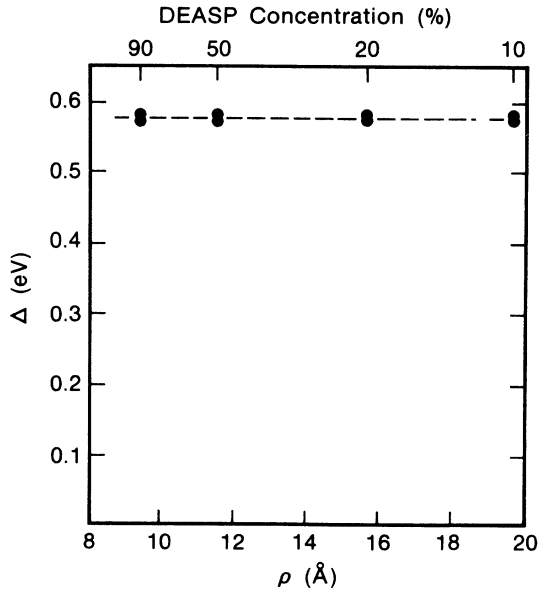

FIG. 9. Zero field activation energy Δ_0 vs intramolecular spacing ρ for the concentration range 10–90 % DEASP:PC for $T < T_g$.

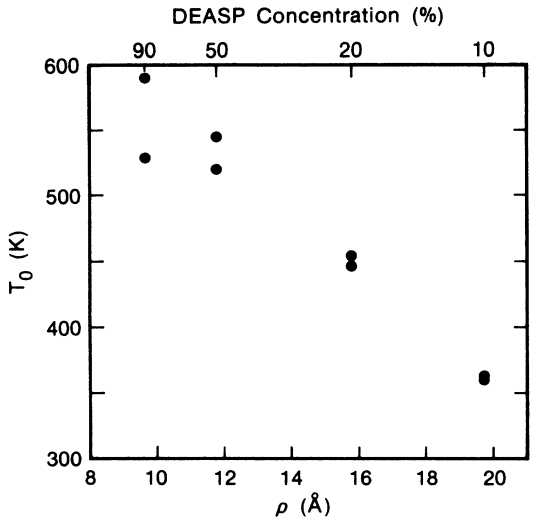

FIG. 10. Plot of the T_0 parameter vs intramolecular spacing for the range 10–90 % DEASP:PC for $T < T_g$.

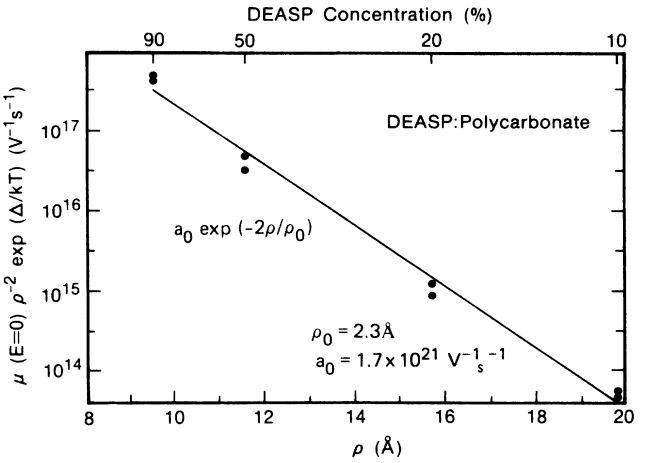

FIG. 12. Plot to determine a_0 and ρ_0 for the DEASP:PC for $T < T_g$. $\mu(E=0)$ is taken at room temperaure. Decay distance $\rho_0 = 2.3$ Å.

ples at the same nominal concentration. The largest errors are due to thickness variations and thickness measurements. However, capacitance measurements tend to average out those errors over the sample effective area.

The drift mobility μ equals $L/E\tau$, where L denotes the sample averaged thickness, τ is the transit time obtained from curves such as Fig. 4, and E is the external electric field applied across the sample. The analysis of the mobility as a function of temperature, electric field, and concentration was performed by the procedure suggested in Ref. 5. From the general empirical Eqs. (1) and (2), one obtains analytically the five parameters, a_0, ρ_0, T_0, β, and Δ_0 by fitting the data points with numerical methods to the following partial derivatives of $\ln\mu$. First, $\ln\mu$ vs $\sqrt{E}$ as a function of T is plotted. S_1, defined as

$$S_1(T,\rho) = \left[\frac{\partial \ln\mu}{\partial(\sqrt{E})}\right]_{T,\rho} = \frac{\beta}{k}\left[\frac{1}{T} - \frac{1}{T_0}\right], \tag{3}$$

can be obtained from the slopes of these curves. The intercepts of the $\ln\mu$ vs $\sqrt{E}$ curves at $E=0$ are used to obtain Δ_0:

$$S_2(E=0,\rho) = \left[\frac{\partial \ln\mu}{\partial(1/T)}\right]_{E,\rho}\Bigg|_{E=0} = -\frac{\Delta_0(\rho)}{k}. \tag{4}$$

Then, using $\Delta_0(\rho)$ and the room-temperature, $E=0$ value

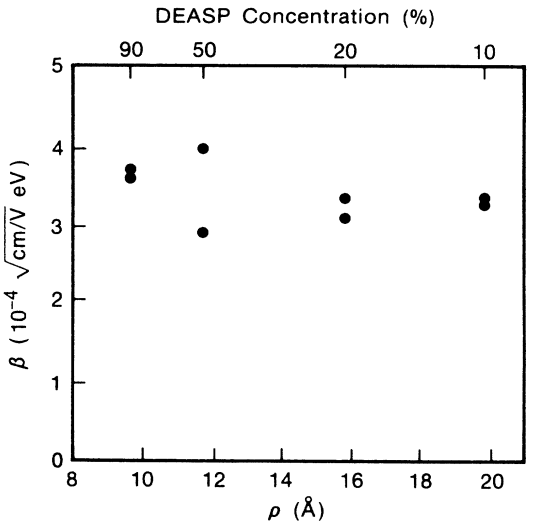

FIG. 11. Plot of the β parameter vs intramolecular spacing for the range 10–90 % DEASP:PC for $T < T_g$.

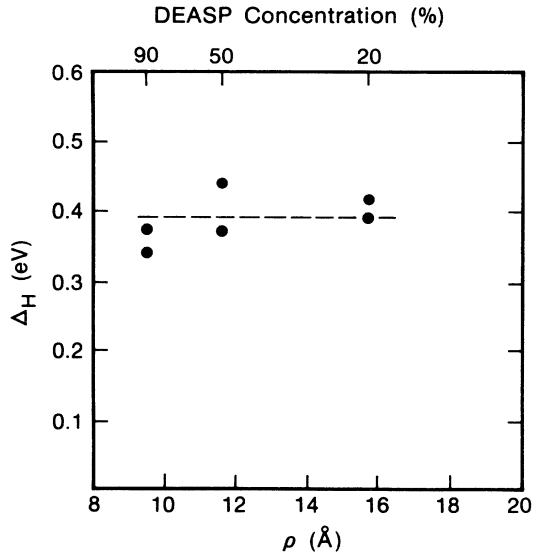

FIG. 13. Zero field activation energy Δ_{0H} for the system DEASP:PC for the concentration range 20–90 % DEASP for $T > T_g$.

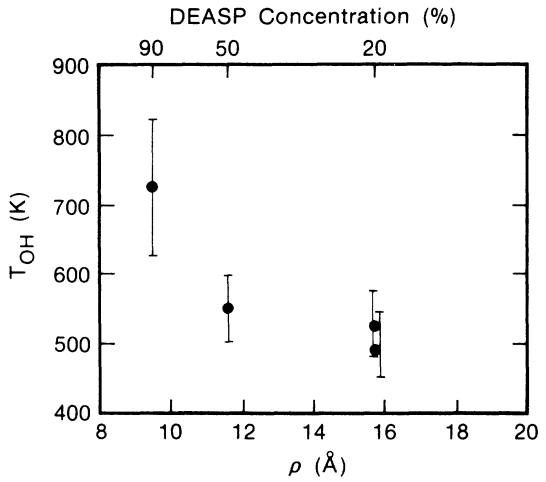

FIG. 14. Plot of the T_{0H} parameter vs intramolecular spacing for the DEASP:PC system in the range 20–90% DEASP for $T > T_g$.

of μ, one may then obtain $\mu_0(\rho)$:

$$\mu(T=295\text{ K}, E=0, \rho)=\mu_0(\rho)\exp\{-[\Delta_0(\rho)/kT]\}\ , \quad (5)$$

where

$$\mu_0=a_0\rho^2\exp(-2\rho/\rho_0)\ . \quad (6)$$

This data analysis procedure, introduced in Ref. 5, allows one to properly deconvolute the dependencies of μ on T, E, and ρ. The dependencies of μ_0 and Δ_0 on ρ offer significant clues to the physical mechanism of hopping.

III. EXPERIMENTAL RESULTS

Figure 5 depicts a typical set of logarithm mobility curves as a function of the square root of the electric field. Using the electric field raised to the $\frac{1}{2}$ power was found to be the best power law for data reported in many MDP systems,[10] including the one reported in this investigation. Since we have extended our mobility measurements above T_g we are able to observe also the change in properties which results from the structural changes at this temperature.[13] Figure 6 shows the zero field mobility (obtained by extrapolation from fig. 5) versus the inverse of the absolute temperature. One observes that at about $T=345$ K the mobility exhibits a breaking point dividing the temperature range into two zones with different zero field activation energies. This breaking point, designated by T_b, is close to the DSC determined glass transition

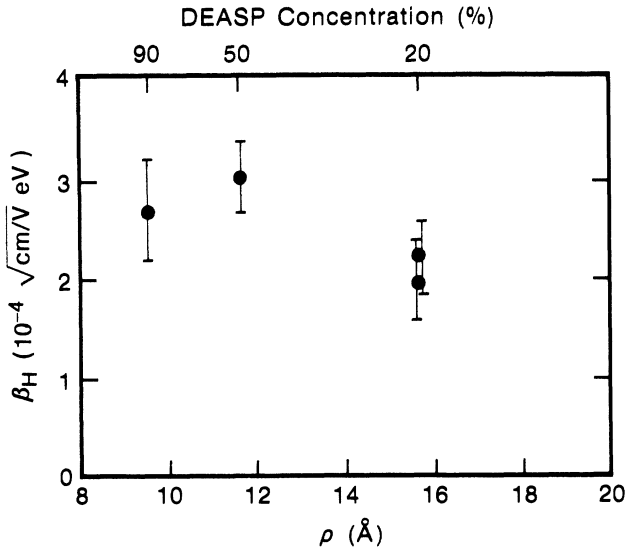

FIG. 15. Plot of β_H parameter for DEASP:PC in the range 20–90% DEASP for $T > T_g$.

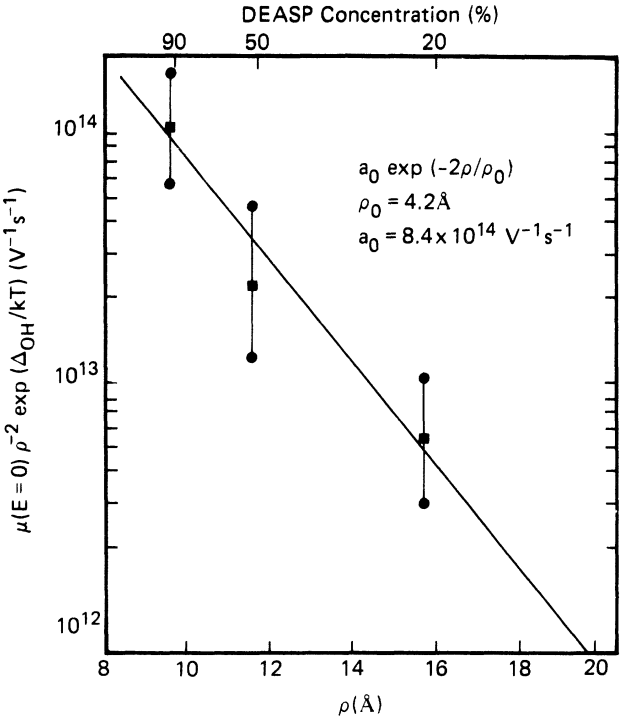

FIG. 16. Plot to determine the a_0 and ρ_0 system for the DEASP:PC for $T > T_g$. Decay distance $\rho_0=4.2$ Å.

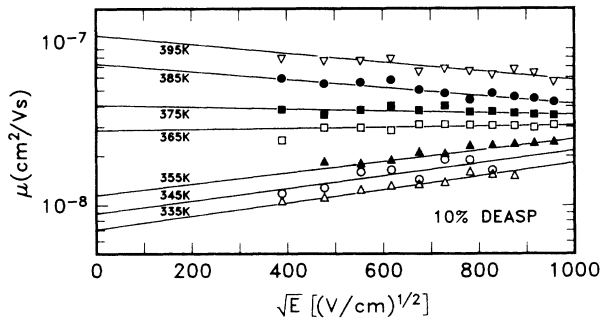

FIG. 17. Hole mobility on 10% DEASP:PC vs square root of electric field. The family of curves is for the temperature range 335–395 K. Note that above 365 K the mobility decreases with an increase of the electric field.

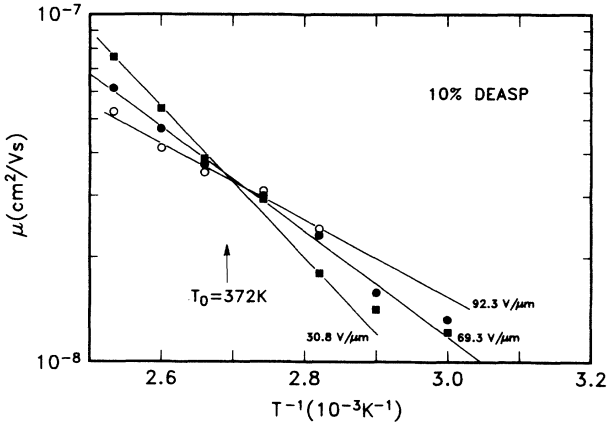

FIG. 18. Data shown in Fig. 17, plotted as $\ln\mu$ vs T^{-1} with E as a parameter. For clarity, only some of the data shown in Fig. 17 are plotted here. Note the curves cross at the temperature at which the mobility becomes field independent; this temperature is called T_0.

temperature which was $T_g = 360$ K for the 50% DEASP:PC samples. In fact, T_b can be seen from Fig. 7 to correspond with T_g as a function of doping concentration.

The values of the parameters β and T_0 are obtained [Eq. (3)] from the slopes of the mobility curves at each temperature of Fig. 5. In Fig. 8, no evidence for a change in the slope of the line at the temperature T_b is observed. Fitting the curve to a straight line gives the parameters β and T_0.

Performing the analysis described above for all DEASP:PC concentrations in the range 10–90 % we obtained the dependencies of $\Delta_\rho(\rho)$, $T_0(\rho)$, $\beta(\rho)$, and $\mu_0(\rho)$ for this system. In Figs. 9–12, we present these functions for the low-temperature zone, i.e., $T < T_g$, and in Figs. 13–16 for the temperature zone $T > T_g$. For the plots with $T > T_g$, the parameters are labeled with an H for high temperature. This method, besides providing a complete functional expression of $\mu(T,E,\rho)$, is also valuable information for probing the physical mechanisms of charge transport in MDP's.

Of special interest were the results obtained for the 10% concentration.[11] At this concentration $T_0 < T_g$ (compared Figs. 3 and 10). It was found that although in the temperature region $T < T_0 \simeq 370$ K the mobility increases exponentially with $\sqrt{E}$, above T_0 this trend is reversed for $T_g > T > T_0$ (see Fig. 17). This means that by some physical phenomenon, the mobility is hindered by the electric field above T_0, although still preserving the same Poole-Frenkel-like $\sqrt{E}$ behavior. That T_0 actually represents a temperature at which the electric field dependence vanishes is clearly shown in Fig. 18, which is a replot of some of the data given in Fig. 17. This is the first time mobility measurements have been made at temperatures above T_0 and still below T_g. The experimental results indicate that Eq. (1) remains applicable even for $T > T_0$. Moreover, with different parameters, Eq. (1) remains valid also for $T > T_g$.

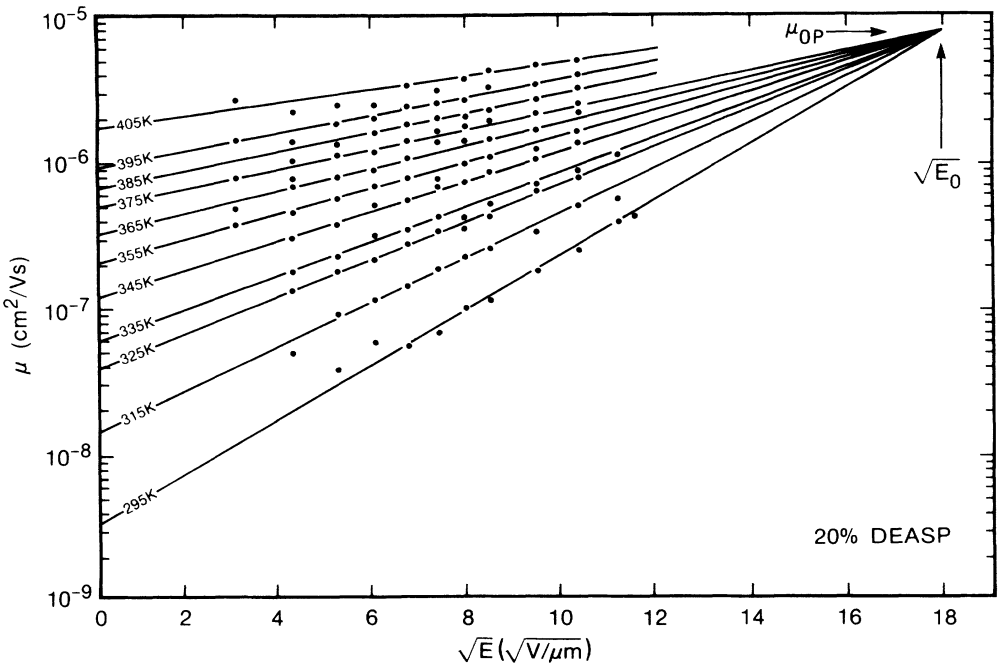

FIG. 19. Mobility curve vs square root of electric field for the 20% DEASP:PC system extrapolated to the field focal point $\sqrt{E_0}$. Observe that in this plot only the curves of $T < T_g$ were used to obtain the value of E_0.

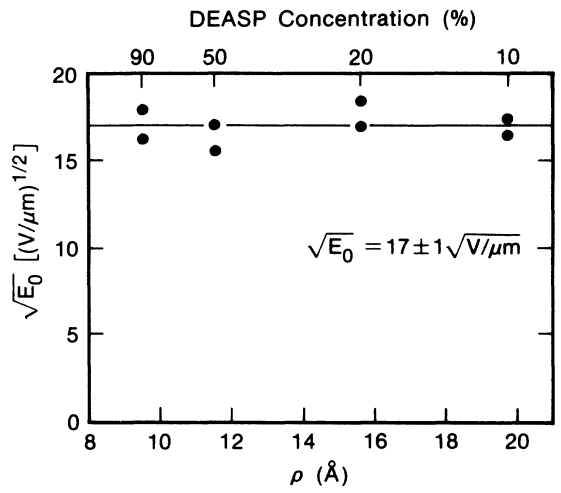

FIG. 20. Plot of $\sqrt{E_0}$ vs ρ for the DEASP:PC system for the doping concentration range of 10–90 %.

IV. DISCUSSION

A. Equivalent empirical formulations of the electrical mobility

Several empirical equations have been suggested in the literature to represent the functional dependencies of the mobilities of electrons and holes in MDP's. In this section we demonstrate their equivalence and the relative advantage of each.

The original equation proposed by Gill[2] is similar to Eq. (1):

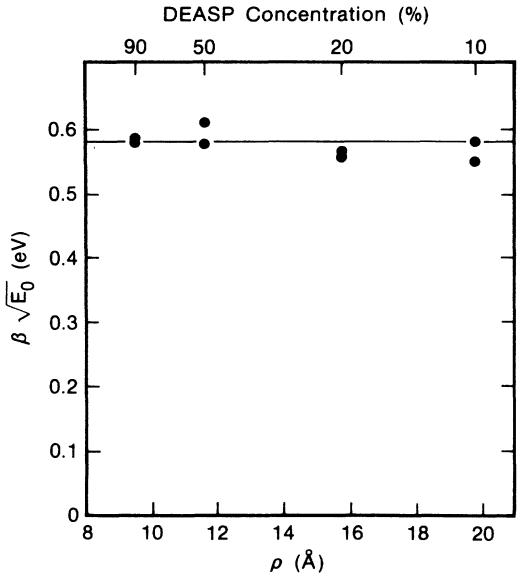

FIG. 21. Plot of the product $\beta\sqrt{E_0}$ for this system. Observe that the result is practically identical with the results in Fig.9 for the $\Delta_0(\rho)$ parameter, i.e., nearly constant value of about 0.58 eV.

$$\mu(T,E,\rho)=\mu_{0G}\exp\left[-(\Delta_0-\beta\sqrt{E})\left[\frac{1}{kT}-\frac{1}{kT_0}\right]\right]. \tag{7}$$

By comparison it can be seen that

$$\mu_0=\mu_{0G}\exp\left[-\frac{\Delta_0}{kT_0}\right], \tag{8}$$

i.e., Gill multiplied the term with T_0 by the term with Δ_0. This led to the definition of an effective temperature T_{eff}:

$$T_{\text{eff}}^{-1}=T^{-1}-T_0^{-1}. \tag{9}$$

and simplification of Eq. (7).

$$\mu(T,E,\rho)=\mu_{0G}\exp[-(\Delta_0-\beta\sqrt{E})/kT_{\text{eff}}]. \tag{10}$$

However, the physical significance of an effective temperature remains unclear.

By contrast, Eq. (1) naturally evolved from the deconvolution techniques discussed earlier[5] and used in Sec. III.

A third equation was suggested by Pfister:[3]

$$\mu=\mu_{0p}\exp\left[\beta(\sqrt{E}-\sqrt{E_0})\left[\frac{1}{kT}-\frac{1}{kT_0}\right]\right], \tag{11}$$

where μ_{0p} and E_0 are new fitting parameters which have the following relationships to the fitting parameters of Eq. (1):

$$\Delta_0=\beta\sqrt{E_0}, \tag{12}$$

$$\mu_{0p}=\mu_0\exp(-\Delta_0/kT_0)=\mu_0\exp\left[\frac{-\beta\sqrt{E_0}}{kT_0}\right]. \tag{13}$$

This equation suggests an alternative procedure for analyzing data. The procedure in this case is to obtain first the focal point at $\sqrt{E_0}$ for all curves of mobility versus $\sqrt{E}$ plots, such as the one given in Fig. 19, for 20% DEASP:PC. The plots for all concentrations allow one to obtain the value of $E_0(\rho)$ as a function of ρ (see Fig. 20). Then, using the plots of $\ln\mu(E=0)$ versus $1/T$ given by Eq. (11), one obtains the values $\beta\sqrt{E_0}(\rho)$ (see Fig.21) from which $\beta(0)$ can be calculated using Eq. (12). The interesting point about Eq. (12) is that the activation energy, Δ_0 at zero field, is given as a product of β and the critical field $\sqrt{E_0}$ (see Fig. 21), a result practically identical with the results of Fig. 9, as expected. This suggests an interpretation of the activation energy Δ_0 as being equivalent to an electric field E_0 at which the mobility becomes temperature independent. Observe that within the experimental error, E_0 has a constant high field value in the range $\sim 3\times 10^7$ V/cm, for the DEASP:PC system, which is beyond the dielectric strength of the material. Preliminary calculations show similar order of magnitude values for all MDP systems[2–7] published in the literature.

A special form of Eq. (1) is one related to the compensation "law" with the electric field as the compensation parameter.[14]

$$\mu=\mu_0\exp\left[\frac{\Delta(E)}{kT_0(\rho)}\right]\exp\left[-\frac{\Delta(E)}{kT}\right], \quad (14)$$

where Δ is defined by

$$\Delta=\Delta_0-\beta\sqrt{E} . \quad (15)$$

The compensation "law" describes the observation that families of Arrhenius curves, plotted versus a compensation variable, intercept at a finite temperature called the compensation temperature. For charge transport in molecularly doped polymers, the compensation variable is the electric field and the compensation temperature is T_0. This empirical "law" has been observed in many other systems. An example includes the dynamics of the photodeposition process. Here the deposition rate of a photoactivated colloid system is studied as a function of temperature and light intensity. The compensation variable is light intensity; a focal point or compensation temperature is observed in the deposition-rate–$(1/T)$ plane. Other examples include self-diffusion of atoms in the solid state and even the intrinsic carrier concentration in semiconductors (with the semiconductor type as the compensation variable). The possibility that these examples of the compensation "law" have a common origin has recently been discussed.[14]

B. Basic theories for electrical transport in MDP's

It appears to be generally accepted that band theory, so successful in describing charge transport in semiconductors and metals, is not useful in insulating materials such as MDP's for at least three reasons. First, the magnitudes of the observed mobilities, 10^{-14}–10^{-9} cm^2/V s, are much too small for band transport.[15] Second, the observed dependence of μ on the distance between dopant molecules, usually observed to be $\exp(-\rho/\rho_0)$ is suggestive of overlap integrals in hopping theories. And third, band theories usually predict a decrease of μ with temperature (as more scattering phonons are created), while mobilities in MDP exponentially increase with temperature.

The only known alternative to band theory, hopping of a localized charge carrier,[16–19] appears to be qualitatively consistent with the data. In this case, the diffusion constant is given by

$$D\sim\rho^2\nu_{el} , \quad (16)$$

where ν_{el} is the electronic hopping rate of the diffusing carrier given by a thermally activated equation

$$\nu_{el}\sim\nu_0\exp(-E_A/kT) . \quad (17)$$

ν_0 is a frequency factor[19] typical of thermal vibrations and E_A is the activation energy, which may depend quite generally on parameters such as electric field and doping concentration. Using the Einstein relationship to obtain the expression for the mobility, one obtains

$$\mu\sim De_{kT}\sim\frac{\nu_0\rho^2 e}{kT}\exp(-E_A/kT) . \quad (18)$$

Inserting typical values into Eq. (18) for the MDP system, i.e., $\nu_0\sim10^{13}$ Hz, $\rho\sim10^{-7}$ cm, and $E_A\simeq0.5$ eV one obtains mobility values in the range 10^{-6}–10^{-8} cm^2/V s for temperatures in the range 295–400 K. These values are obtained experimentally in many systems. Therefore, at least qualitatively, this justifies the use of the diffusional hopping model of charge barriers between localized sites in MDP's.

Unfortunately, this expression is obtained quite generally for almost all hopping theories.[16–19] Therefore, without more information, it is not possible to distinguish among these theores in order to understand the microscopic details of the hopping process occurring in MDP's.

Recently, additional information has been obtained by Schein and co-workers[5] that suggests small polaron motion may be occurring in these materials. There are two small polaron regimes of interest.[17] One is the adiabatic small polaron regime which occurs when, given an energy coincidence between two neighboring hopping sites, the probability of a polaron making the hop is unity. In this case, the mobility is

$$\mu_{\text{adiabatic}}\simeq\mu_0\rho^2\exp\{-[E_p/2-J(\rho)/kT]\} , \quad (19)$$

where $E_p/2$ is one-half of the polaron binding energy and J is the overlap integral which is a function of hopping distance. The other regime is called the nonadiabatic small polaron regime which occurs when the above-mentioned probability is less than 1. Here the mobility is

$$\mu_{\text{nonadiabatic}}\simeq\mu_0\rho^2\exp(-2\rho/\rho_0)\exp(-E_p/2kT) . \quad (20)$$

The main characteristics of this regime are that the activation energy does not depend on dopant concentration or intramolecular distance ρ and μ contains the overlap dependence, i.e., $\exp(-2\rho/\rho_0)$. In contrast, for the adiabatic regime, the activation energy depends on ρ through J, but the overlap term, i.e., $\exp(-2\rho/\rho_0)$ is just unity. It is this difference in behavior that was found by Schein and co-workers in two MDP's after correct data analysis.[5,20]

DEASP:PC appears to exhibit the characteristic of nonadiabatic small polaron hopping. Note in Fig. 9 that the activation energy is constant 0.58 eV, independent of ρ, and in Fig. 12 that μ_0 is exponential in ρ, with $\rho_0=2.3$ Å below T_g.

C. The electric field dependence

As can be seen in Figs. 5 and 19, $\ln\mu$ appears to be described within experimental error by $\sqrt{E}$. This result appears to be quite general; recent statistical analysis[10] over a wider E field range in hydrazone:PC gave the same result. However, attempts to understand this result have not been successful, as is described elsewhere.[10]

The first experimental mobility measurements above T_0 are shown in Fig. 17 for 10% DEASP:PC. For this system, $T_0=370$ K and $T_g=398$ K allowing measurements between T_0 and T_g. The important experimental result obtained is the observation that above T_0 the mobility decreases as a function of increasing electric field.

Also, the field dependence $\exp\sqrt{E}$ remains the same above T_0. These surprising characteristics are predicted mathematically by all of the empirical equations [(1), (7), (11), and (14)]. They are, however, inconsistent with the predictions of Bässler[21] and Hirsch.[22] Bässler[21] suggested that T_0 is an artifact resulting from the way data were being plotted ($\ln\mu$ versus T^{-1} instead of $\ln\mu$ versus T^{-2}). This suggestion appeared resonable since T_0 had been obtained by a long extrapolation on $\ln\mu$ versus T^{-1} plots with E as a parameter. However, Fig. 18, which is a plot of the same data given in Fig. 17 but on $\ln\mu$ versus T^{-1} axes, clearly demonstrates T_0 is not an artifact. Hirsch[22] suggested the appearance of a T_0 parameter may be the result of a temperature-dependent dielectric constant. He predicted the E field curves on a $\ln\mu$ versus T^{-1} should deviate from straight lines so as to come together above T_0, also inconsistent with the data shown in Fig. 18.

D. The mobility above T_g for DEASP:PC

Most charge-transport investigations of MDP materials in the past have been made below the glass transition temperature T_g. However, from a theoretical point of view, one is interested in whether the same formalism expressed by Eq. (1) and the polaron theory Eqs. (19) and (20) can be extended to include the mobility characteristics above T_g.

Clearly, as seen in Fig. 6, there is a change in activation energy at a temperature T_b, which correlates with the glass transition temperature (Fig. 7), in agreement with earlier measurements.[13] From Fig. 8 it is seen that S_1, which is used to obtain the two electric field parameters T_0 and β, does not appear to change at T_b. Comparing Figs. 9–11 with Figs. 13–15 shows that while Δ_0 significantly changes at the glass transition temperature, T_0 and β, within experimental error, do not. This is the first material system in which the observation of the constance of T_0 and β as T is raised above the glass transition temperature is reported. Data with smaller error bars would be useful to further check the conclusion. This result appears to be consistent with other data reported in this paper and in an earlier work.[5] These data show that T_0 decreases with ρ, opposite to the behavior of T_g on ρ (compare Figs. 10 and 14 with Fig. 3 and see Ref. 5). Such data were used to suggest that T_0 is not associated with rheological properties of the materials. It appears that it may be possible to strengthen this conclusion: the overall electric field dependence appears not to be associated with the rheological properties of the material.[23] The value of these parameters for DEH, DEASP, and TPD molecularly doped polymers are shown in Table I.

From Figs. 13 and 16 we observe that even above T_g the DEASP:PC system still exhibits the nonadiabatic behavior, i.e., $\Delta_{0H}(\rho)\simeq$const and the $\exp(-2\rho/\rho_{0H})$ dependence. However, $\Delta_{0H}\simeq 0.38$ eV, only about $\frac{2}{3}$ of the value observed below T_g (0.58 eV) (see Figs. 9 and 13). From Figs. 12 and 16, we find the ρ_0 parameter is 2.3 Å below T_g and significantly larger, 4.2 Å, above T_g. μ_0 (calculated at 11.5 Å) is $\approx 10^3$ cm^2/V s below T_g but only ≈ 0.05 cm^2/V s above T_g. These results suggest that the activation energy, ρ_0 and μ_0, depend partially on the complex structure of the polymer matrix rather than being connected solely with the dopant molecule. The differences can be ascribed to new degrees of freedom acquired by a particle diffusing through a glassy matrix which is heated above its T_g. It is well known that above T_g the polymer molecules acquire translational motion besides the vibrational and thermal flipping motion which exist below T_g. The much larger value of ρ_{0H} as compared to ρ_0 suggest that the delocalization of the charge carriers in MDP's depends on the ability of the host matrix molecuels to access various thermally excitated modes at a particular temperature. It is, therefore, very important to investigate how the vibrational, rotational, and translational modes of thermal excitation in the polymeric matrix are involved in the electrical hopping motion of charge carriers. This investigation, however, is beyond the scope of this publication.

The large value of μ_0 below T_g, $\approx 10^3$ cm^2/V s in this sytem is of interest. It has been conjectured that the $E=0, T=\infty$ limit of the mobility, i.e., μ_0, is the limiting value for a microscopic hopping mobility process in a disordered material. Typical observed values in other systems are below 10^{-1} cm^2/V s, as is our value of μ_0 above T_g. Such small values are lower than are expected for band theories consistent with the conjective. Howev-

TABLE I. The five empirical parameters describing DEH:DC, DEASP:PC, and TDP:PC. The hole mobilities in DEH is an abbreviation for *p*-diethylaminobenzaldehyde-diphenyl hydrazone; TPD is an abbreviation for *N,N'*-diphenyl-*N,N'*-bis (3-methylphenyl)-[1,1'-biphenyl]-4,4'-diamine.

a_0 ($V^{-1}s^{-1}$)	ρ_0 (Å)	Δ (eV) (% dopant conc.)	β (eV $\sqrt{\text{cm/V}}$)	T_0 (K) (% dopant conc.)	
1.25×10^{23}	1.7	0.6	3.5×10^{-4}	510–380 (90–10)	DEH $T<T_g$
1.7×10^{21}	2.3	0.58	3.5×10^{-4}	556+30 to 370 (90–10)	DEASP $T<T_g$
8.4×10^{14}	4.2	0.4	3×10^{-4}	720±100 to 500±40 (90–20)	DEASP $T>T_g$
1.2×10^{5}		0.2–0.53 (90–20)			TPD $T<T_g$

er, this new observation of a μ_0 as large as 10^3 cm^2/V s would seem to indicate the conjective is incorrect.

V. CONCLUSION

We have investigated the hole mobility in the DEASP:PC system as a function of electric field, temperature, and the dopant molecular concentration. It is shown that the empirical equation, suggested previously, describes the data below as well as above the glass transition temperature. In terms of the equation

$$\mu=a_0\rho^2\exp[-(2\rho/\rho_0)]\exp(-\Delta_0/kT) \times\exp\left[\beta\sqrt{E}\left[\frac{1}{kT}-\frac{1}{kT_0}\right]\right] \quad (21)$$

the parameters for DEH:PC, DEASP:PC below T_g and above T_g, and TPD:PC are given in the table. Note that the value of Δ_0, a_0, and ρ_0 change above T_g. In contrast, the data appear to suggest that the parameters describing the electric field dependence, β and T_0, do not change above T_g. Data over a wider concentration range with smaller errors bars would be useful to further check this potentially important conclusion. Δ_0 and ρ_0 change at T_g presumably due to an increase in the degrees of freedom of the polymer matrix. At a dopant concentration of 10% DEASP, an important feature appeared above T_0: the hole mobilities decrease as the electric field increases. This result verifies that T_0 is a real parameter, not an artifact of the way data were being plotted. This first direct observation of T_0 demonstrates that two available theories of T_0 are inconsistent with our data. The electric field dependence for the hole mobility in this sytem was found to be of the form $\exp\sqrt{E}$ below and above T_g consistent with previously suggested empirical equations. A new result is that this field dependence seems to hold even for the zone above T_0 where it was shown that the mobility decreases as a function of increasing electric field, thereby creating an "inverted" Poole-Frenkel-like effect.

ACKNOWLEDGMENTS

The authors wish to express their gratitude to C. R. Peled for her extensive programming performed in the course of this investigation.

*Present address: Center for Technological Education affiliated with Tel-Aviv University, 58368 Holon, Israel.

[1]L. B. Schein, *Electrophotography and Development Physics* (Springer-Verlag, New York, 1988).
[2]W. G. Gill, J. Appl. Phys. **43**, 5033 (1972).
[3]G. P. Pfister, Phys. Rev. B **16**, 3676 (1977).
[4]M. Stolka, J. F. Janus, and D. M. Pai, J. Phys. Chem. **88**, 4707 (1984).
[5]J. X. Mack, L. B. Schein, and A. Peled, Phys. Rev. B **39**, 7500 (1989).
[6]M. Stolka, in *Electrical and Electronic Properties of Polymers,* edited by J. I. Kroschwitz (Wiley, New York, 1987), p. 301.
[7]J. Mort, G. Pfister, and S. Grammatica, Solid State Commun. **18**, 693 (1976).
[8]R. Hesse and H. Bässler, Phys. Status Solidi B **101**, 481 (1980).
[9]L. B. Schein, A. Rosenberg, and S. L. Rice, J. Appl. Phys. **60**, 4287 (1986).
[10]L. B. Schein, A. Peled, and D. Glatz, J. Appl. Phys. **66**, 686 (1989).
[11]A. Peled and L. B. Schein, Chem. Phys. Lett. **153**, 422 (1988).
[12]P. J. Melz, R. B. Champ, L. S. Chang, C. Chiou, G. S. Keller, L. C. Liclican, R. R. Neiman, M. D. Shattuck, and W. J. Weiche, Photogr. Sci. Eng. **21**, 73 (1977).
[13]M. Abkowitz, M. Stolka, and M. Morgan, J. Appl. Phys. **52**, 3453 (1981).
[14]A. Peled and L. B. Schein, J. Appl. Phys. D (to be published).
[15]R. H. Bube, *Electronic Properties of Crystalline Solids* (Academic, New York, 1974), p. 254; S. H. Glarum, J. Phys. Chem. Solids **24**, 1577 (1963).
[16]H. Böttger and V. V. Bryskin, *Hopping Conduction in Solids* (Akademie-Verlag, Berlin, 1985).
[17]D. Emin, in *Electronics and Structural Properties of Amorphous Semiconductors,* edited by P. G. LeComber and J. Mort (Academic, New York, 1973), Chap. 7.
[18]P. Nagels, in *Amorphous Semiconductors,* edited by M. H. Brodsky (Springer-Verlag, Berlin, 1979), p. 113–158.
[19]D. Adler, *Amorphous Semiconductors* (CRC, Cambridge, 1971).
[20]L. B. Schein and J. X. Mack, Chem. Phys. Lett. **149**, 109 (1988).
[21]H. Bässler, Philos. Mag. B **50**, 347 (1984).
[22]J. Hirsch, J. Phys. C **12**, 321 (1979).
[23]M. Fujino, Y. Kanazawa, H. Mikawa, S. Kusabayashi, and M. Yokotana, Solid State Commun. **49**, 575 (1984).